

Purinergic signalling is required for calcium oscillations
in migratory chondrogenic progenitor cells

Csaba Matta · János Fodor · Nicolai Miosge ·
Roland Takács · Tamás Juhász · Henrik Rybaltovszki ·
Adrienn Tóth · László Csernoch · Róza Zákány

Received: 2 March 2014 / Revised: 26 April 2014 / Accepted: 5 May 2014
© Springer-Verlag Berlin Heidelberg 2014

Abstract Osteoarthritis (OA) is the most common form of chronic musculoskeletal disorders. A migratory stem cell population termed chondrogenic progenitor cells (CPC) with in vitro chondrogenic potential was previously isolated from OA cartilage. Since intracellular Ca^{2+} signalling is an important regulator of chondrogenesis, we aimed to provide a detailed understanding of the Ca^{2+} homeostasis of CPCs. In this work, CPCs immortalised by lentiviral administration of the human telomerase reverse transcriptase (hTERT) and grown in monolayer cultures were studied. Expressions of all three IP_3Rs were confirmed, but no RyR subtypes were detected. Ca^{2+} oscillations observed in CPCs were predominantly dependent on Ca^{2+} release and store replenishment via store-operated Ca^{2+} entry; CPCs express both STIM1 and Orai1 proteins. Expressions of adenosine receptor mRNAs were verified, and adenosine elicited Ca^{2+} transients. Various

P2 receptor subtypes were identified; $P2Y_1$ can bind ADP; $P2Y_4$ is targeted by UTP; and ATP may evoke Ca^{2+} transients via detected P2X subtypes, as well as $P2Y_1$ and $P2Y_2$. Enzymatic breakdown of extracellular nucleotides by apyrase completely abrogated Ca^{2+} oscillations, suggesting that an autocrine/paracrine purinergic mechanism may drive Ca^{2+} oscillations in these cells. As CPCs possess a broad spectrum of functional molecular elements of Ca^{2+} signalling, Ca^{2+} -dependent regulatory mechanisms can be supposed to influence their differentiation potential.

Keywords SOCE · Calcium oscillation · Osteoarthritis · Mesenchymal stem cell · Chondrogenesis

Abbreviations

2-APB	2-Aminoethoxydiphenyl borate	43
ARC	Arachidonic acid-regulated Ca^{2+} channel	46
CPA	Cyclopiazonic acid	48
CPC	Chondrogenic progenitor cell	50
CRAC	Calcium release activated Ca^{2+} channel	53
ESC	Embryonic stem cell	53
FTHM	Full time at half maximum	56
HDC	High density cell culture	58
hTERT	Human telomerase reverse transcriptase	60
IP_3R	Inositol 1,2,3-trisphosphate receptor	63
MSC	Mesenchymal stem cell	63
NCX	Sodium calcium exchanger	66
OA	Osteoarthritis	68
PBST	Phosphate-buffered saline with Tween 20	70
PG	Proteoglycan	73
PMCA	Plasma membrane Ca^{2+} -ATPase	73
RyR	Ryanodine receptor	76
SDS-PAGE	Sodium dodecyl sulphate polyacrylamide gel electrophoresis	78
SERCA	Sarcoplasmic/endoplasmic reticulum Ca^{2+} -ATPase	82

Csaba Matta and Janos Fodor contributed equally to the work.

Electronic supplementary material The online version of this article (doi:10.1007/s00424-014-1529-8) contains supplementary material, which is available to authorized users.

C. Matta · R. Takács · T. Juhász · R. Zákány (✉)
Department of Anatomy, Histology and Embryology, Faculty of
Medicine, University of Debrecen, Nagyerdei krt. 98,
H-4032 Debrecen, Hungary
e-mail: roza@anat.med.unideb.hu

J. Fodor · A. Tóth · L. Csernoch
Department of Physiology, Faculty of Medicine, University of
Debrecen, Nagyerdei krt. 98, H-4032 Debrecen, Hungary

N. Miosge
Research Group for Oral Biology and Tissue Regeneration, Faculty
of Medicine, Department of Prosthodontics, Georg August
University, 37075 Goettingen, Germany

H. Rybaltovszki
Department of Orthopaedics, Faculty of Medicine, University of
Debrecen, Nagyerdei krt. 98, H-4032 Debrecen, Hungary

83 SOCE Store-operated Ca^{2+} entry
86 STIM Stromal interacting molecule

89 Introduction

90 The global prevalence of musculoskeletal disorders (compris-
91 ing more than 200 conditions and syndromes, including var-
92 ious rheumatic, arthritic and joint diseases) is constantly rising
93 owing to unfavourable changes in the population of developed
94 countries (i.e. higher incidence of obesity, increased mean
95 age). Osteoarthritis (OA) is the most common chronic form
96 of conditions affecting articular cartilage. In the initial, largely
97 asymptomatic stages of the disease, the homeostatic balance
98 between cartilage matrix synthesis and degradation is lost
99 [38]. At the clinical stage, inflammation of the synovial mem-
100 brane is often present, which further influences chondrocyte
101 metabolism to enhance catabolism and reduce anabolism,
102 resulting in altered extracellular matrix (ECM) homeostasis
103 and composition [32]. Indeed, OA-affected cartilage matrix
104 has long been known to undergo profound changes in terms of
105 collagen, glucosaminoglycan and water content [31], which in
106 turn alters the osmolarity of the matrix and its unique ionic
107 milieu, and affects chondrocyte metabolism [30]. While alter-
108 ations of OA-affected cartilage matrix components and com-
109 position have been investigated in detail, the cellular nature of
110 the disease has not been sufficiently characterised.

111 We have recently documented a distinct cell population
112 with migratory potential in OA-affected articular cartilage
113 [25]. These chondrogenic progenitor cells (CPCs) exhibit
114 certain stem cell surface markers and possess stem cell-like
115 characteristics such as clonogenicity, multipotency and migra-
116 tory activity. CPCs express intermediate levels of both the
117 osteogenic and chondrogenic transcription factors Runx2 and
118 Sox9, respectively, indicating that they are likely derived from
119 the osteochondroprogenitor lineage [25].

120 Although CPCs *in vivo* have only limited regeneration
121 capacity, a better understanding of their biological character-
122 istics and targeted manipulation of certain pathways may lead
123 to enhanced synthesis and regeneration of cartilage ECM.
124 However, knowledge concerning their physiological proper-
125 ties is almost completely lacking. Since arthritic cartilage
126 matrix undergoes profound changes especially at the late
127 stages of the disease, it is logical to assume that cells in OA-
128 affected cartilage may be characterised by a unique assembly
129 of plasma membrane ion channels and transporters that regu-
130 late their function and phenotype and consequently maintain
131 communication with the extracellular space. Indeed, accord-
132 ing to a genome-wide analysis that compared the mRNA
133 transcriptome of chondrocytes isolated from articular cartilage
134 of healthy and OA patients, the expression of several plasma
135 membrane ion channels with a putative role in volume

regulation, apoptosis, and proliferation was found to be sig- 136
nificantly altered [20]. 137

138 Based on the above findings, it can be hypothesised that 138
alterations of the molecular “calcium toolkit” that regulates 139
 Ca^{2+} homeostasis are also present in inflammatory 140
chondrocytes and other cell types in OA-affected cartilage. 141
Indeed, NMDA receptors with altered subunit composition 142
and activity were described in OA chondrocytes [44]; further- 143
more, intracellular calcium oscillations associated with inor- 144
ganic calcium crystal-induced cartilage matrix degradation 145
were also observed [40]. These alterations can serve as a 146
background for modified metabolism and altered physiologi- 147
cal properties of these cells. In particular, ATP is also known 148
to be an important mediator in various inflammatory condi- 149
tions; more specifically, ATP levels can significantly increase 150
following its release by damaged cells [9]. In turn, elevated 151
levels of ATP provoke the activation of purinergic receptors, 152
mainly P2X and P2Y receptors [3]. In particular, synovial 153
fibroblasts obtained from OA patients were reported to ex- 154
press P2X₁ and P2X₃ receptors at high density that modulated 155
some functional responses closely associated with inflamma- 156
tion [52]. 157

158 In light of these data, we aimed to provide a detailed 158
understanding of the Ca^{2+} homeostasis in undifferentiated, 159
proliferating CPCs immortalised by lentiviral administration 160
of hTERT and grown in monolayer. We characterised calcium 161
influx functions through the plasma membrane with special 162
emphasis on purinergic signalling; furthermore, we also 163
mapped Ca^{2+} release pathways from internal Ca^{2+} stores, as 164
well as Ca^{2+} elimination functions. Moreover, the contribution 165
of these pathways to the regulation of low-frequency sponta- 166
neous Ca^{2+} oscillations is also discussed. 167

168 Materials and methods

169 Cell cultures

170 CPCs were isolated, immortalised and cultured as described 170
earlier [25]. Briefly, adult osteoarthritic cartilage, without 171
signs of rheumatoid involvement, was obtained from the knee 172
joints of patients (ages 65–75 years) suffering from late-stage 173
OA after total knee replacement. Standard explant cultures 174
were performed using 8–15-mm³ tissue specimens taken from 175
areas adjacent to the main defect. After 10 days, outgrown 176
cells were harvested, and 10³ cells · cm⁻² were transferred to a 177
monolayer culture in Dulbecco’s modified Eagle’s medium 178
(DMEM; Sigma-Aldrich, St. Louis, MO, USA; pH 7.4) with 179
10 % foetal bovine serum (FBS; Gibco, Gaithersburg, MD, 180
USA), supplemented with penicillin/streptomycin (50,000 U/ 181
50 mg) and L-glutamine (10 mM), and cultured under standard 182
conditions. Immortalisation of CPCs was carried out by co- 183
transfection of plasmid pLenti6/v5-hTERT with pLP1, pLP2 184

185 and pLP/VSVG helper plasmids (ViraPower lentiviral expres- 236
186 sion system, Invitrogen, Karlsruhe, Germany) into 293FT 237
187 cells, and the supernatant was collected after 48 h. P1 CPCs 238
188 were infected with hTERT lentivirus (moi $5 \cdot 10^4$) and selected 239
189 with $10 \text{ mg} \cdot \text{mL}^{-1}$ blasticidin for 1 week. 240

190 In these experiments, the CPC531 clone cultured in mono- 241
191 layer was used. CPCs were routinely maintained in 75-cm^2 242
192 cell culture flasks (Orange Scientifique, Braine-l'Alleud, Bel- 243
193 gium) in DMEM containing $1 \text{ g} \cdot \text{L}^{-1}$ glucose and 10 % FBS 244
194 until approximately 80 % confluence and were passaged. For 245
195 calcium measurements, cells were harvested and transferred 246
196 onto 30-mm round coverslips (Menzel-Gläser, Menzel 247
197 GmbH, Braunschweig, Germany) placed into 35-mm plastic 248
198 Petri dishes (Orange Scientifique) at a density of $10^3 \text{ cells} \cdot$ 249
199 cm^{-2} . Cultures were used only until they reached approxi- 250
200 mately 80 % confluence. For RT-PCR and Western blot anal- 251
201 yses, cells were grown in 150-cm^2 tissue culture dishes (Or- 252
202 ange Scientifique) until approximately 80 % confluency and 253
203 were then harvested. The medium was changed on every 254
204 second day. 255

205 To confirm that cells used in this study retained their 256
206 osteochondroprogenitor nature at the level of their tran- 257
207 scriptome, we performed chondrogenic (*Sox9*, *Col2a1*, *Acan*) 258
208 and osteogenic (*Runx2*, *Col1a1*, *Col10a1*) marker gene ex- 259
209 pression analysis using RT-PCR (for details, see Table S1 and 260
210 Fig. S1 given in the Online Resource). 261

211 Single cell fluorescent Ca^{2+} measurements

212 Measurements were performed using the calcium-dependent 262
213 fluorescent dye Fura-2 as described previously [11]. Briefly, 263
214 cultures were transferred to 1 mL of fresh DMEM containing 264
215 $5 \mu\text{L}$ of Fura-2-acetoxymethyl ester (AM; $10 \mu\text{M}$; Life Tech- 265
216 nologies, Carlsbad, CA, USA) and $3 \mu\text{L}$ of neostigmin 266
217 (0.3 nM ; to inhibit extracellular choline-esterase activity; 267
218 TEVA, Debrecen, Hungary) and incubated in a CO_2 incubator 268
219 at 37°C for 1 h. Fura-2-loaded cells were then placed on the 269
220 stage of an inverted fluorescent microscope (Diaphot; Nikon, 270
221 Kowasaki, Japan) and viewed using a $40\times$ oil immersion 271
222 objective. Calcium imaging was performed in normal 272
223 Tyrode's (containing 137 mM NaCl , 5.4 mM KCl , 0.5 mM 273
224 MgCl_2 , 1.8 mM CaCl_2 , 11.8 mM HEPES ; $1 \text{ g} \cdot \text{L}^{-1}$ glucose; 274
225 pH 7.4) or in Ca^{2+} -free Tyrode's solution (containing 5 mM 275
226 EGTA, without CaCl_2). Excitation wavelength was altered 276
227 between 340 and 380 nm (F_{340} and F_{380}) by a 277
228 microcomputer-controlled dual-wavelength monochromator 278
229 equipment (DeltaScan; Photon Technologies International, 279
230 New Brunswick, NJ, USA). Emission was detected at 280
231 510 nm at a 10-Hz acquisition rate using a photomultiplier. 281
232 Background fluorescence was subtracted online from F_{340} and 282
233 F_{380} signals by the data acquisition software. 283

234 Intracellular $[\text{Ca}^{2+}]$ was calculated from the ratio of mea- 284
235 sured fluorescence intensities ($R = F_{340}/F_{380}$) as described by

Grynkiewicz and colleagues [14]. The measuring bath was 236
constantly perfused with normal Tyrode's solution at a rate of 237
 $2 \text{ mL} \cdot \text{min}^{-1}$ (EconoPump; Bio-Rad Laboratories, CA, USA). 238
Test solutions were directly applied to the cells through a 239
perfusion capillary tube (Perfusion Pencil™; AutoMate Sci- 240
entific, San Francisco, CA, USA) with an internal diameter of 241
 $250 \mu\text{m}$ at a rate of $1.5 \mu\text{L} \cdot \text{s}^{-1}$, using a local perfusion system 242
(Valve Bank™ 8 version 2.0, AutoMate Scientific). All mea- 243
surements were performed at room temperature. 244

245 Solutions and drugs

246 Single cell calcium measurements were performed in normal 247
or Ca^{2+} -free Tyrode's solutions (see above). All compounds 248
were purchased from Sigma-Aldrich. The aspecific IP_3R in- 249
hibitor 2-aminoethoxydiphenyl borate (2-APB) [2] ($75 \mu\text{M}$) 250
was diluted in 0 mM Ca^{2+} Tyrode's (stock: 1 M in DMSO); 251
the non-specific TRPC antagonist YM-58483 (a pyrazole 252
derivative; also known as BTP-2) [15] ($1 \mu\text{M}$) and the 253
aspecific Ca^{2+} influx channel blocker LaCl_3 [24] ($500 \mu\text{M}$) 254
were diluted in normal (1.8 mM Ca^{2+}) Tyrode's solution 255
(stocks: 1 mM and 300 mM in distilled water and DMSO, 256
respectively). The sarcoplasmic/endoplasmic reticulum Ca^{2+} - 257
ATPase (SERCA) inhibitor cyclopiazonic acid (CPA; $10 \mu\text{M}$) 258
[27] was diluted in Ca^{2+} -free Tyrode's solution (stock: 10 mM 259
in DMSO). Caffeine (30 mM), which was used in this study to 260
increase the sensitivity of ryanodine receptor (RyR) for calc- 261
ium, or as an antagonist of P1 adenosine receptors [42], was 262
dissolved in 1.8 mM Ca^{2+} Tyrode's. The general P2X and 263
P2Y purinergic receptor agonist ATP ($180 \mu\text{M}$) was dissolved 264
in both 0 and 1.8 mM Ca^{2+} Tyrode's; agonists of P2Y 265
purinergic receptors (ADP, UTP and UDP; all $100 \mu\text{M}$) were 266
dissolved in 1.8 mM Ca^{2+} Tyrode's. The aspecific P2X and 267
P2Y purinergic receptor inhibitor suramin ($10 \mu\text{M}$) [43] was 268
dissolved in both 0 and 1.8 mM Ca^{2+} Tyrode's. The P1 269
receptor agonist adenosine ($100 \mu\text{M}$) was prepared in 270
 1.8 mM Ca^{2+} Tyrode's. To catalyse the hydrolysis extracellu- 271
lar ATP to AMP, apyrase ($5 \text{ U} \cdot \text{mL}^{-1}$) diluted in Ca^{2+} -free 272
Tyrode's was applied.

273 mRNA expression analysis using reverse transcription 274 followed by PCR (RT-PCR)

275 Subconfluent colonies of CPC cells cultured in 150-cm^2 plas- 276
tic cell culture dishes were washed three times with RNase- 277
free physiological NaCl, dissolved in TRIzol (Applied 278
Biosystems, Foster City, CA), and following the addition of 279
 20% RNase-free chloroform (Sigma-Aldrich) samples were 280
centrifuged at $10,000\times g$ for 15 min at 4°C . Total RNA- 281
containing samples were incubated in $500\text{-}\mu\text{L}$ RNase-free 282
isopropanol at -20°C for 1 h , total RNA was dissolved in 283
nuclease-free water (Promega, Madison, WI, USA) and stored 284
at -70°C .

285 The composition of the assay mixture (20 μ L) for reverse
286 transcriptase (RT) reactions was as follows: 1,000-ng total
287 RNA; 0.25- μ L RNase inhibitor; 2- μ L random primers;
288 0.8- μ L dNTP Mix (4 mM); 50 units (1 μ L) of MultiScribe™
289 RT in 1 \times RT buffer (High Capacity RT kit; Applied
290 Biosystems, Foster City, CA, USA). cDNA was transcribed
291 at 37 °C for 2 h.

292 Amplifications of specific cDNA sequences were carried
293 out using specific primer pairs that were designed by Primer
294 Premier 5.0 software (Premier Biosoft, Palo Alto, CA, USA)
295 based on human nucleotide sequences published in GenBank
296 and purchased from Integrated DNA Technologies, Inc. (IDT;
297 Coralville, IA, USA). The specificity of custom-designed
298 primer pairs was confirmed in silico by using the Primer-
299 BLAST service of NCBI ([http://www.ncbi.nlm.nih.gov/
300 tools/primer-blast/](http://www.ncbi.nlm.nih.gov/tools/primer-blast/)). Nucleotide sequences of forward and
301 reverse primers and reaction conditions are shown in
302 Table S2 in the Online Resource. PCR reactions were
303 carried out in a final volume of 25 μ L containing 1–1- μ L
304 forward and reverse primers (10 μ M), 0.5- μ L cDNA, 0.5- μ L
305 dNTP Mix (200 μ M), and 1 unit (0.2 μ L) of GoTaq® DNA
306 polymerase in 1 \times Green GoTaq® Reaction Buffer (Promega)
307 in a programmable thermal cycler (Labnet MultiGene™ 96-
308 well Gradient Thermal Cycler; Labnet International, Edison,
309 NJ, USA) with the following protocol: 2 min at 95 °C for
310 initial denaturation followed by 35 repeated cycles of dena-
311 turation at 94 °C for 30 s, primer annealing for 45 s at an
312 optimised temperature for each primer pair (see Table S2 in
313 the Online Resource) and extension at 72 °C for 90 s. After the
314 final cycle, further extension was allowed to proceed for
315 another 7 min at 72 °C. PCR products were analysed using
316 horizontal gel electrophoresis in 1.2 % agarose gels containing
317 ethidium bromide at 100 V constant voltage.

318 SDS–PAGE and Western blot analysis

319 Total lysates of CPCs for electrophoresis (SDS–PAGE) were
320 prepared as described previously [11], with minor modifica-
321 tions for subconfluent cell cultures. Briefly, cultures were
322 washed with physiological NaCl solution and were harvested.
323 After centrifugation at 2,000 \times g for 10 min at room tempera-
324 ture, cell pellets were suspended in 100 μ L of RIPA homog-
325 enisation buffer containing 150 mM NaCl, 1.0 % NP40, 0.5 %
326 sodium deoxycholate, 50 mM Tris, 0.1 % sodium dodecyl
327 sulphate (SDS; pH 8.0), supplemented with protein inhibitors
328 as follows: aprotinin (10 μ g \cdot mL⁻¹), 5 mM benzamidine,
329 leupeptin (10 μ g \cdot mL⁻¹), trypsin inhibitor (10 μ g \cdot mL⁻¹),
330 1 mM phenylmethylsulfonyl fluoride (PMSF), 5 mM EDTA,
331 1 mM EGTA, 8 mM Na-fluoride and 1 mM Na-
332 orthovanadate. All components were purchased from Sigma-
333 Aldrich. Samples were stored at -70 °C. Suspensions were
334 sonicated by pulsing burst for three times 30 s by 50 cycles
335 using an ultrasonic homogeniser (Cole-Parmer, Vernon Hills,

IL, USA). Samples for SDS–PAGE were prepared by adding 336
1/5 volume of 5 \times concentrated Laemmli's electrophoresis 337
sample buffer (310 mM Tris–HCl; pH 6.8, 10 % SDS, 50 % 338
glycerol, 100 mM DTT, 0.01 % bromophenol blue) to cell 339
lysates and heated at 95 °C for 5 min. 340

Protein 50 μ g was separated by 7.5 % SDS–PAGE gel for 341
immunological detection of key proteins involved in Ca²⁺- 342
homeostasis of CPC cells. Proteins were transferred to nitro- 343
cellulose membranes by using a Bio-Rad Trans-Blot Turbo 344
system (Bio-Rad, Hungary). After blocking in 5 % non-fat dry 345
milk in PBS, membranes were incubated with primary anti- 346
bodies overnight at 4 °C as shown in Table S3 in the Online 347
Resource. After washing for 30 min in PBST, membranes 348
were incubated with the HRP-conjugated secondary antibod- 349
ies, anti-rabbit or anti-mouse IgG (Bio-Rad) in 1:1,500 dilu- 350
tion. Membranes were developed by enhanced chemilumines- 351
cence reaction (Millipore, Billerica, MA, USA) according to 352
the instructions of the manufacturer. 353

354 Statistical analysis

All data are representative of at least three independent exper- 355
iments. Averages are expressed as mean \pm SEM (standard 356
error of the mean; *n*, number of cells measured). Statistical 357
analysis was performed by using Student's *t* test. Threshold 358
for statistically significant differences as compared to respec- 359
tive control cultures was set at **P*<0.05. 360

361 Results

Spontaneous Ca²⁺ transients in CPCs are mediated by internal 362
stores via IP₃R 363

The dynamics of intracellular Ca²⁺ levels in CPCs was 364
analysed in Fura-2-loaded cells during 1,000-s long intervals. 365
In the majority of cells observed during single cell Ca²⁺ 366
measurements in standard (containing 1.8 mM Ca²⁺) bath 367
solution (in 20 of 28 cells; 71 %), spontaneous Ca²⁺ transients 368
were observed, with considerable individual variations in 369
frequency and amplitude among cells (Fig. 1a, c, d). The 370
average frequency of transients was $1.3 \times 10^{-3} \pm 1.3 \times$ 371
 10^{-4} Hz; the amount of Ca²⁺ liberated during each transient 372
was $23.6 \pm 5.4 \mu\text{M} \cdot \text{s}$; the average amplitude of Ca²⁺ spikes 373
was $116.6 \pm 11.6 \text{ nM}$; and the rate of rise of transients was 2.2 374
 $\pm 0.5 \text{ nM} \cdot \text{s}^{-1}$ (in each case, *n*=20) (Fig. 1c, d). 375

To establish whether the primary source of elevated cyto- 376
solic Ca²⁺ levels was an influx through plasma membrane 377
Ca²⁺ channels or a release from internal Ca²⁺ stores (e.g. the 378
ER), further experiments were performed. When CPCs were 379
bathed in Ca²⁺-free Tyrode's during single cell Ca²⁺ measure- 380
ments, spontaneous Ca²⁺ transients were still detectable (in 9 381
of 10 cells investigated; 90 %), although with gradually 382

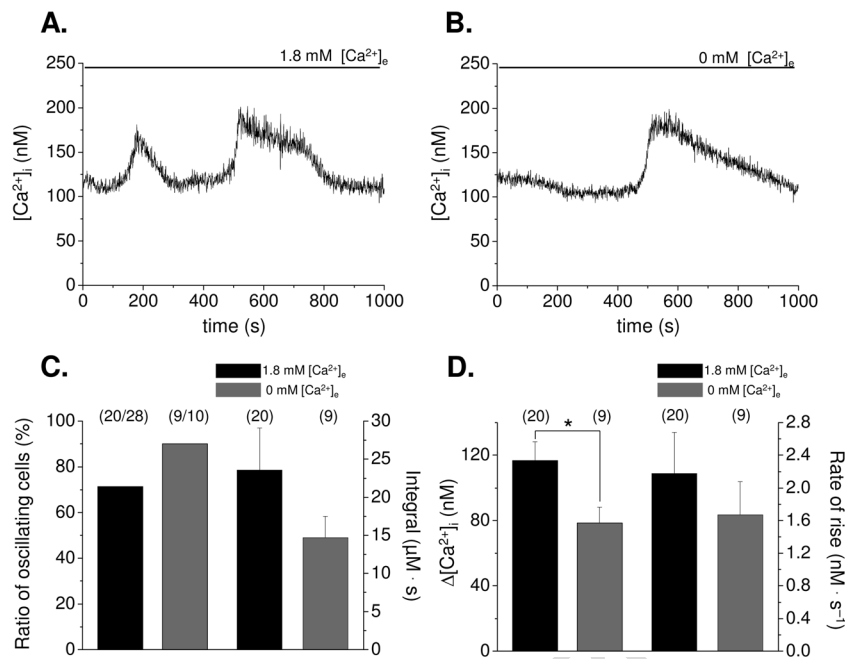


Fig. 1 Spontaneous Ca^{2+} oscillations in CPCs and pooled data demonstrating the different parameters of the phenomenon. **a** Ca^{2+} oscillations detected without agonist stimulation in standard Tyrode's solution containing 1.8 mM Ca^{2+} Tyrode's at room temperature. Representative record of Fura2-AM-loaded cells analysed during 1,000-s long intervals. **b** Ca^{2+} oscillations detected without agonist stimulation in Ca^{2+} -free Tyrode's at room temperature. Representative record of Fura2-AM-

loaded cells analysed during 1,000-s long intervals. **c** Ratio of oscillating cells and integral of Ca^{2+} transients. Numbers in parentheses above bars indicate the number of cells measured. **d** Mean values of the amplitude and the rate of rise of transients (calculated as $d[\text{Ca}^{2+}]_i/dt$). Numbers in parentheses above bars indicate the number of cells measured. Asterisks (*) mark significant ($P<0.05$) differences between cells bathed in standard and Ca^{2+} -free Tyrode's

decreasing amplitudes and frequencies (Fig. 1b, d). The average frequency and amplitude of these spikes were $1.4 \times 10^{-3} \pm 1.5 \times 10^{-4}$ Hz and 78.5 ± 9.8 nM, respectively, and $14.7 \pm 2.8 \mu\text{M} \cdot \text{s}$ Ca^{2+} was found to be released during each Ca^{2+} transient. The rate of rise of transients was $1.7 \pm 0.4 \text{ nM} \cdot \text{s}^{-1}$ (in each case, $n=9$) (Fig. 1c, d). While significant differences were found between the amplitudes of transients in Ca^{2+} -free medium compared to controls ($P=0.02$), neither the amount of liberated Ca^{2+} nor the rate of rise of the transients were statistically different ($P=0.26$ and $P=0.49$, respectively; Fig. 1c, d). These results suggested that although a Ca^{2+} influx through plasma membrane ion channels contributed to the amplitude of Ca^{2+} spikes, the primary source of Ca^{2+} to generate spontaneous Ca^{2+} transients could probably be the internal stores.

To confirm this claim, further experiments were carried out. First, we investigated to what extent internal stores contributed to the generation of Ca^{2+} spikes. When the SERCA inhibitor CPA (10 μM) was added to the bath solution with 1.8 mM Ca^{2+} and concurrent inhibition of store-operated Ca^{2+} entry (SOCE) by LaCl_3 (500 μM) and YM-58483 (1 μM) was applied, spontaneous activity was completely abolished ($n=10$). This observation suggested that even though Ca^{2+} was available extracellularly, the fact that internal stores were depleted and store replenishment was concurrently blocked was sufficient to completely abrogate spontaneous transients,

which supported the idea that the function of internal Ca^{2+} stores was of key importance in this process. To test the role of IP_3 receptors, the cell-permeable aspecific IP_3R blocker 2-APB (75 μM) was administered to the bath solution during single cell Ca^{2+} measurements with no external Ca^{2+} available. In this case, no spontaneous activity could be detected ($n=10$), which implicated that Ca^{2+} release through IP_3R subtype(s) was required for the induction of transient rise in cytosolic Ca^{2+} . In contrast, application of 30 mM caffeine had no effect on spontaneous Ca^{2+} events, nor did it evoke changes in resting Ca^{2+} levels ($n=10$), suggesting no important regulatory function of RyRs.

Functional characterisation of internal Ca^{2+} stores

Since according to the above results, IP_3R in the ER membrane seemed to play a determining role in generating Ca^{2+} transients, we undertook to characterise the internal Ca^{2+} stores. First, by using specific primer pairs, we performed an mRNA transcript analysis of key molecules involved in Ca^{2+} release and re-uptake and found that although all three IP_3R isoforms were observed in CPCs, no specific bands for RyR subtypes could be detected (Table 1). We also screened molecules that orchestrate SOCE and found that both isoforms of the ER Ca^{2+} sensor molecule STIM (STIM1 and STIM2) and all three isoforms of the plasma membrane CRAC channel

Table 1 mRNA expression of molecules involved in Ca^{2+} homeostasis of CPCs

Gene	Band detected at expected amplicon size
A. Ca^{2+} release	
<i>IP₃R Type 1</i>	+
<i>IP₃R Type 2</i>	+
<i>IP₃R Type 3</i>	+
<i>RyR 1</i>	–
<i>RyR 2</i>	–
<i>RyR 3</i>	–
B. Store-operated Ca^{2+} entry (SOCE)	
<i>Orai1</i>	+
<i>Orai2</i>	+
<i>Orai3</i>	+
<i>STIM1</i>	+
<i>STIM2</i>	+
C. Ca^{2+} extrusion	
<i>PMCA1</i>	+
<i>PMCA2</i>	–
<i>PMCA3</i>	–
<i>PMCA4</i>	+
<i>NCX1</i>	+
<i>NCX2</i>	–
<i>NCX3</i>	+
<i>NCX4</i>	–
D. Ca^{2+} re-uptake	
<i>SERCA1</i>	+
<i>SERCA2</i>	+
<i>SERCA3</i>	+
E. P1 purinergic receptors	
<i>A₁</i>	+
<i>A_{2A}</i>	+
<i>A_{2B}</i>	+
<i>A₃</i>	–
F. P2X ionotropic purinergic receptors	
<i>P2X₁</i>	+
<i>P2X₂</i>	–
<i>P2X₃</i>	–
<i>P2X₄</i>	+
<i>P2X₅</i>	+
<i>P2X₆</i>	+
<i>P2X₇</i>	+
F. P2Y metabotropic purinergic receptors (G_q-coupled)	
<i>P2Y₁</i>	+
<i>P2Y₂</i>	+
<i>P2Y₄</i>	+
<i>P2Y₆</i>	+
<i>P2Y₁₁</i>	+

Orai (Orai1, Orai2 and Orai3) mRNAs were expressed by CPCs (Table 1).

Having confirmed the presence of mRNA transcripts of these molecules, the next step was to identify their protein level expression. By applying isotype-specific IP_3R anti-sera, all IP_3R subtypes ($\text{IP}_3\text{R1}$, $\text{IP}_3\text{R2}$ and $\text{IP}_3\text{R3}$) were found to be expressed by CPCs as revealed by Western blot analyses (Fig. 2a). Of the molecules that orchestrate SOCE, only STIM1 and Orai1 were detectable at the protein level (Fig. 2a).

The functionality of these proteins was investigated during single cell fluorescent Ca^{2+} recordings (Fig. 2b, d). When the SERCA blocker CPA (10 μM) was administered to cells in Ca^{2+} -free Tyrode's, an approximately 60 nM rise in resting Ca^{2+} levels was observed, caused by Ca^{2+} release from the internal stores probably via IP_3Rs and concurrent inhibition of Ca^{2+} re-uptake, followed by a stable decline owing to the activity of Ca^{2+} elimination pathways other than SERCA (i.e. plasma membrane Ca^{2+} ATPase, PMCA or $\text{Na}^+-\text{Ca}^{2+}$ exchanger, NCX; mRNA expressions are shown in Table 1). From these data, the releasable Ca^{2+} content of internal Ca^{2+} stores could be calculated, which was $22.2 \pm 2.4 \mu\text{M} \cdot \text{s}$ ($n=25$). This data is in a good correlation with what has been described in various other cell types [4]. When the bath solution was replaced by 1.8 mM Ca^{2+} -containing Tyrode's, a large (approx. 150 nM) transient Ca^{2+} influx was detected in response to depleted internal stores, demonstrating store-operated Ca^{2+} entry (SOCE; Fig. 2b, c). When the experiment was repeated with concurrent application of non-specific SOCE blockers YM-58483 (1 μM) and LaCl_3 (500 μM), a significantly smaller amplitude ($\Delta[\text{Ca}^{2+}]_i$: 131.0 ± 16.4 nM vs. 69.2 ± 10.6 nM; $n=13$ and 8; $P=0.005$) was recorded after Ca^{2+} became available in the bath solution; however, the differences in rate of rise (2.0 ± 0.5 nM $\cdot \text{s}^{-1}$ vs. 0.9 ± 0.2 nM $\cdot \text{s}^{-1}$; $n=13$ and 8; $P=0.16$) were not statistically significant (Fig. 2b, d). This is probably a consequence of large individual variations among cells.

Extracellular administration of nucleotides evoke Ca^{2+} transients in CPCs

Given that our results implicate the dependence of spontaneous fluctuations in cytosolic Ca^{2+} on the activation of internal Ca^{2+} stores via IP_3R , we aimed to identify signalling pathways that couple extracellular signals to the IP_3R . Since periodic Ca^{2+} transients in human mesenchymal stem cells (MSCs) could be attributed to an autocrine/paracrine purinergic signalling loop [22], and as the ionotropic purinoreceptor P2X_4 was proved to play a role in differentiation of chicken chondroprogenitor cells [10], we hypothesised the presence of a similar purinergic signal transduction mechanism also in migratory chondroprogenitor cells. To investigate the possibility of such regulatory systems, we first carried out a comprehensive mRNA transcript screening for all purinergic

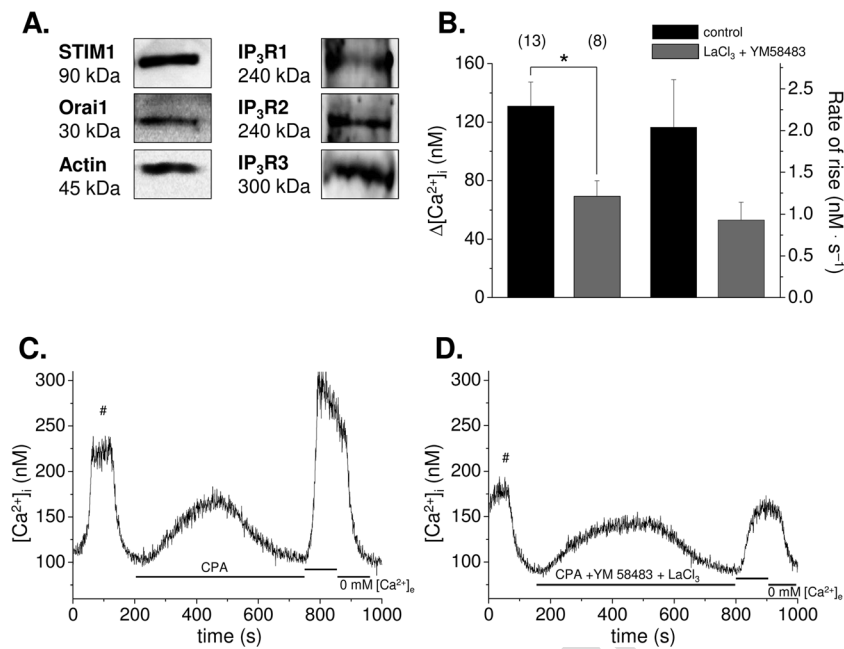


Fig. 2 Functional investigation of internal Ca²⁺ stores in CPCs. **a** Protein expression of molecules (STIM1 and Orai1) that orchestrate the SOCE mechanism and isoforms of the Ca²⁺ release channel of internal stores (IP₃R1, IP₃R2 and IP₃R3). Actin was used as a control. Representative data of three independent experiments. **b** Pooled data of amplitudes and rate of rise of transients evoked by Ca²⁺ entry after the re-administration of external calcium. Numbers in parentheses indicate the number of cells measured. Asterisks (*) mark significant (*P < 0.05) differences between the control and cells pre-treated with LaCl₃ and YM-58483. **c** Store-operated Ca²⁺ entry (SOCE) in Fura-2-loaded CPCs during single cell fluorescent Ca²⁺ imaging. Internal Ca²⁺ stores of cells were previously

depleted by the application of 10 μM CPA in Ca²⁺-free Tyrode's for 500–600 s, which caused a prominent increase in $[Ca^{2+}]_i$. When $[Ca^{2+}]_e$ was changed back to normal (1.8 mM), a large transient increase in $[Ca^{2+}]_i$ was observed, demonstrating SOCE. Representative record. Hashmark (#) indicates spontaneous Ca²⁺ transients at the beginning of measurements. **d** Store-operated Ca²⁺ entry (SOCE) in Fura-2-loaded CPCs during single cell fluorescent Ca²⁺ imaging in the presence of SOCE inhibitors 500 μM LaCl₃ and 1 μM YM-58483. Hashmark (#) indicates spontaneous Ca²⁺ transients at the beginning of measurements. Representative record

receptor mRNAs involved in Ca²⁺ homeostasis and found that of the A1 adenosine receptor subtypes A₁, A_{2A} and A_{2B}, but not A₃ adenosine receptor transcripts; of the P2X ionotropic purinergic receptor subtypes P2X₁, P2X₄, P2X₅, P2X₆ and P2X₇, but not P2X₂ and P2X₃; and mRNAs for all G_q-coupled P2Y metabotropic purinergic receptor subtypes were detectable using RT-PCR (see Table 1; mRNA expression of other P2Y receptor subtypes are shown in the Online Resource in Table S4 and Fig. S2).

To assess the functionality of these receptors, P1 and P2 receptor agonists were administered to CPCs during single cell calcium measurements. When the effect of ATP (180 μM), a general P2 receptor agonist, was tested, rapid and large amplitude (338.1 ± 28.5 nM; n = 44), repetitive Ca²⁺ transients could be detected in normal (1.8 mM $[Ca^{2+}]_e$) Tyrode's solution (n = 44 of 48 cells; 91 %), reflecting on the activity of P2 purinergic receptors (Fig. 3a; Table 2). The average duration of transients expressed as full time at half maximum (FTHM) values was 16.1 ± 2.6 s. When ATP was administered in 0 mM external Ca²⁺, repetitive transients could still be evoked (n = 35 of 36 cells; 97 %; Fig. 3b), but with significantly lower amplitudes compared to the control (204.6 ± 25.0 nM; n = 35; P = 0.0009; Fig. 3d). Similarly, there was a statistically significant

difference between the rate of rise of transients in control and Ca²⁺-free solutions (72.9 ± 12.6 nM · s⁻¹ vs. 35.4 ± 8.8 nM · s⁻¹; P = 0.02; Fig. 3e). However, no change was observed in the duration of transients (20.6 ± 3.1 s; P = 0.29).

The above data suggested the contribution of both ionotropic P2X and metabotropic P2Y purinergic receptors and/or SOCE. However, when the IP₃R inhibitor 2-APB was co-applied with ATP, transients could be evoked only in a few cases (n = 2 of 19 cells; 10 %; Fig. 3c), raising the possibility that mainly metabotropic P2Y receptor activity could be accounted for the observed Ca²⁺ transients or that 2-APB could aspecifically block Ca²⁺ influx. To confirm these hypotheses, further experiments were conducted.

Having suggested the key role of P2Y receptors in the Ca²⁺ homeostasis of CPCs, we undertook to further characterise their precise involvement in generating Ca²⁺ transients upon agonist stimulation. To this end, the effects of various P2Y receptor agonists were tested during single cell Ca²⁺ measurements (see Table 2). While UTP (100 μM) and ADP (100 μM) evoked prominent Ca²⁺ transients (324.5 ± 20.5 and 284.0 ± 25.0 nM, respectively) in most of the cells examined (n = 13 of 15 and 18 of 20 cells, respectively), no response was detected when UDP (100 μM) was administered to cells

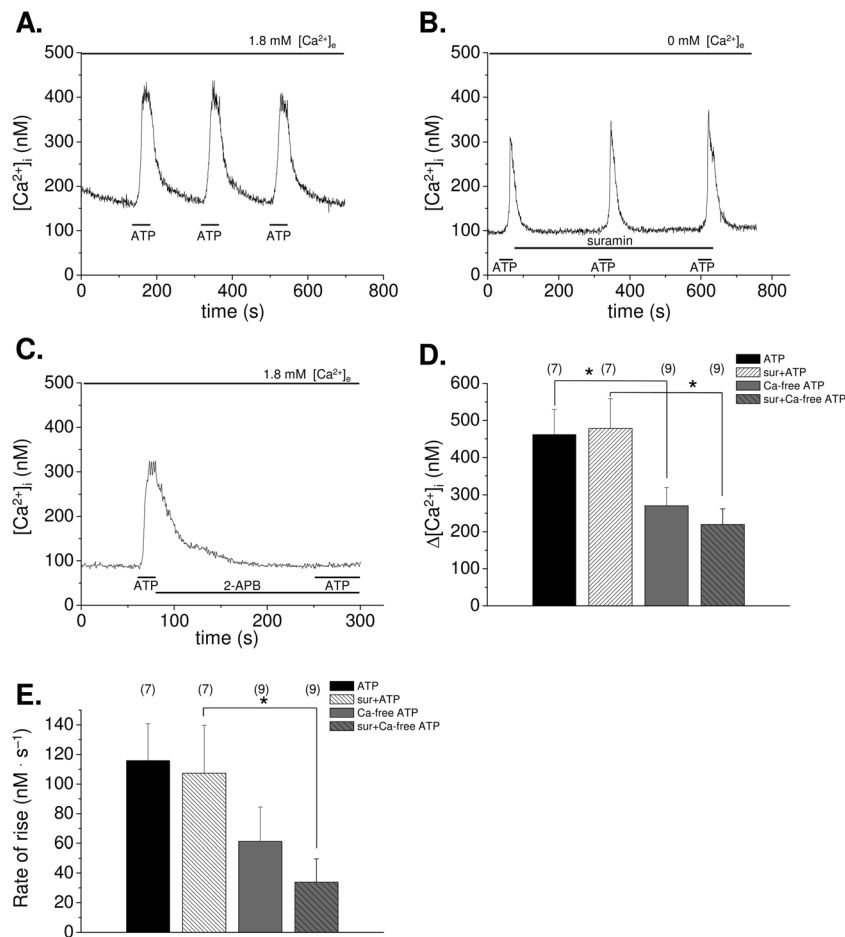


Fig. 3 Functional characterisation of P2 purinergic receptors in CPCs. **a** Calcium transients elicited by repeated administration of ATP in the presence of external calcium. Representative record. **b** Effect of the non-specific P2 purinergic antagonist suramin (10 μ M) on ATP-evoked calcium transients in the absence of external calcium. Representative trace. **c** Representative record showing the lack of ATP-evoked Ca^{2+} transients in the presence of the aspecific IP_3R inhibitor 2-APB in 1.8 mM Ca^{2+} -containing Tyrode's. **d** Changes in the amplitude of ATP-evoked calcium transients detected in 1.8 mM Ca^{2+} -containing and Ca^{2+} -

free Tyrode's. Ca^{2+} transients recorded before suramin application were considered as controls. Numbers in parentheses show the number of cells measured. Asterisk (*) marks a significant ($*P < 0.05$) difference between cells bathed in standard and Ca^{2+} -free solutions. **e** Changes in the rate of rise of ATP-evoked calcium transients detected in 1.8 mM Ca^{2+} -containing and Ca^{2+} -free Tyrode's. Ca^{2+} transients recorded before suramin application were considered as controls. Numbers in parentheses show the number of cells measured. Asterisk (*) marks a significant ($*P < 0.05$) difference between cells bathed in standard and Ca^{2+} -free solutions

($n=0$ of 11 cells; Fig. 4a, c, e). Furthermore, the functionality of P1 adenosine receptors was also confirmed as local

application of adenosine (100 μ M) evoked Ca^{2+} transients (average amplitude 258.5 ± 26.7 nM) in most of the cells

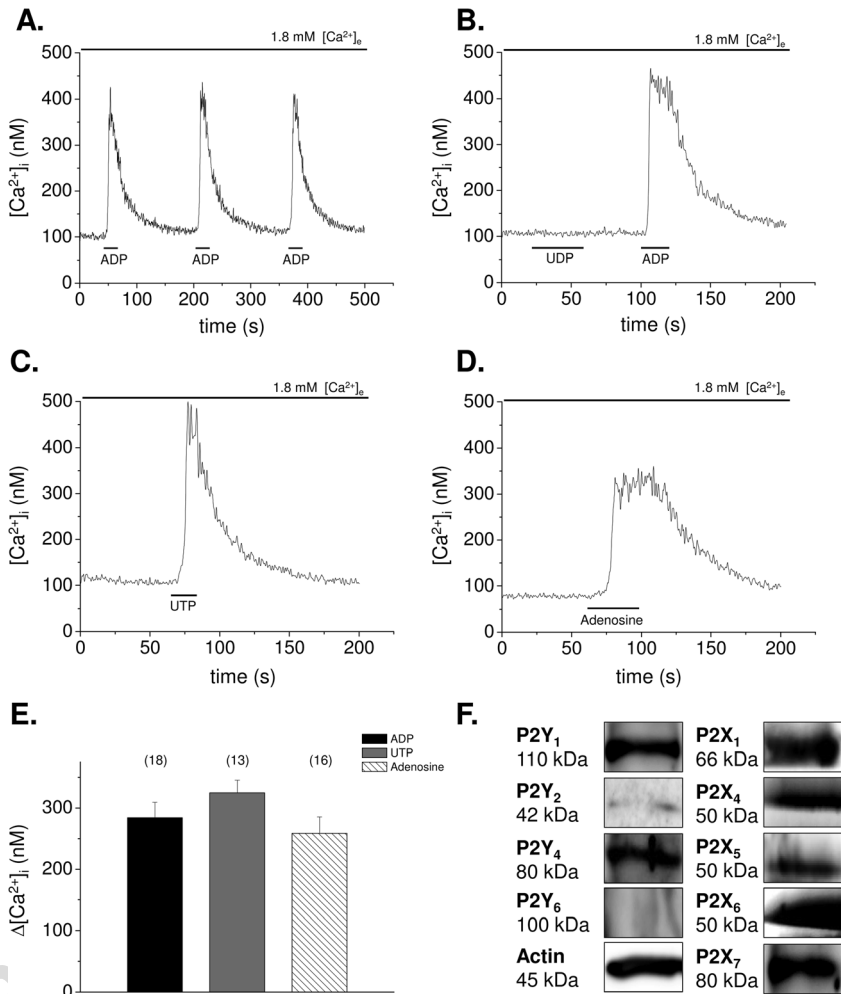
Table 2 Minimum (resting) and maximum Ca^{2+} concentration values, transient amplitudes and transient durations expressed as full time at half maximum (FTHM) values during agonist stimulation (ATP, 180 μ M; ADP, 100 μ M; UTP, 100 μ M; Ade, 100 μ M) of CPCs

		$[Ca^{2+}]_{i, \min}$ (nM) ^a	$[Ca^{2+}]_{i, \max}$ (nM) ^a	Amplitude (nM) ^a	FTHM (s) ^a
t2.3	ATP, 180 μ M ($[Ca^{2+}]_i=1.8$ mM), $n=44$	121.2 \pm 3.5	452.8 \pm 28.9	338.2 \pm 28.6	16.1 \pm 2.6
t2.4	ATP, 180 μ M ($[Ca^{2+}]_i=0$ mM), $n=35$	97.0 \pm 4.2	301.7 \pm 27.0	204.6 \pm 25.0	20.6 \pm 3.1
t2.5		$P=2.8 \cdot 10^{-7}$ *	$P=0.0002$ *	$P=0.0009$ *	$P=0.29$ *
t2.6	ADP, 100 μ M ($[Ca^{2+}]_i=1.8$ mM), $n=18$	112.0 \pm 3.1	396.1 \pm 24.9	284.1 \pm 25.0	24.1 \pm 2.5
t2.7	UTP, 100 μ M ($[Ca^{2+}]_i=1.8$ mM), $n=13$	98.2 \pm 3.9	422.8 \pm 23.2	324.6 \pm 20.50	23.0 \pm 2.6
t2.8	Ade, 100 μ M ($[Ca^{2+}]_i=1.8$ mM), $n=16$	119.6 \pm 11.5	378.1 \pm 34.6	258.5 \pm 26.7	23.0 \pm 3.2

* P values refer to differences between ATP transients elicited in Tyrode's containing 0 mM vs. 1.8 mM Ca^{2+} (Student's t test)

^aData are expressed as mean \pm standard error of the mean (SEM)

Fig. 4 Functional characterisation of P1 and P2Y receptors. **a** Effect of repetitive application of 100 μ M ADP on Ca^{2+} transients measured in the presence of external calcium. Horizontal lines indicate the application of ADP. Representative trace. **b** Representative record showing that 100 μ M UDP was ineffective to evoke Ca^{2+} transients in the presence of external calcium. **c** Calcium transient elicited by administration of UTP in the presence of external calcium. Representative trace. **d** 100 μ M adenosine-evoked Ca^{2+} transient measured in the presence of external calcium proving the functionality of A1 receptors in CPCs. Representative record. **e** Average values of amplitudes for each nucleotide-evoked Ca^{2+} transient. Data represent mean \pm standard error of the mean (SEM). Numbers in parentheses above bars indicate the number of cells measured. **f** Western blot analysis of purinergic receptor subtypes. Total protein samples were used (30 μ g in each lane) to examine the protein expression level. Actin was used as a control. Representative data of three independent experiments



investigated ($n=16$ of 18 cells; Fig. 4d), while co-application of adenosine with the P1 receptor blocker caffeine (30 mM) eliminated this response ($n=0$ of 10 cells). The average duration of transients elicited by these agonists was approximately the same. Table 2 summarises the main parameters of agonist-induced transients (i.e. minimum and maximum cytosolic Ca^{2+} concentrations, amplitudes and durations expressed as FTHM values).

Functional expression of P2 purinergic receptors

As mentioned earlier, mRNAs of various P2 purinergic receptor subunits were detected in the transcriptome of CPCs (see Table 1). Next, we applied immunoblot analyses to confirm the presence of these molecules at the protein level. Of the P2Y receptors, only the G_q protein-coupled P2Y receptor subtypes (i.e. P2Y₁, P2Y₂, P2Y₄, P2Y₆ and P2Y₁₁) were investigated in this study. While all five P2X ionotropic purinergic receptor subtypes were confirmed, only P2Y₁ and P2Y₄ could be identified, and the P2Y₂ receptor protein was weakly expressed in total cell lysates of CPCs (Fig. 4f).

Uncropped Western blot images are shown in the Online Resource (Figs. S3, S4 and S5).

To rule out the function of certain P2X and P2Y receptors, the non-specific P2 receptor antagonist suramin (10 μ M) was administered prior to and during local application of P2 receptor agonists. As seen in Fig. 3b, d, e, none of the parameters of Ca^{2+} transients evoked by ATP either in 1.8 or 0 mM Ca^{2+} -containing Tyrode's were altered by the presence of suramin, indicating that mainly suramin-insensitive P2 purinergic receptors (i.e. P2X₄, P2X₆ and/or P2Y₄) were responsible for the observed effects.

Since Ca^{2+} oscillations in hMSCs are known to be mediated by an autocrine/paracrine purinergic signalling loop, we also wanted to confirm whether repetitive Ca^{2+} transients in CPCs were linked to the function of purinergic receptors. When apyrase, an enzyme that catalyses the hydrolysis of ATP to AMP and inorganic phosphate, was administered to cells prior to and during single cell Ca^{2+} measurements at 5 U mL^{-1} concentration, no repetitive Ca^{2+} transients were observed ($n=5$), implicating the requirement of extracellular ATP for the initiation of Ca^{2+} oscillations in CPCs.

574 Discussion

575 Dynamics of cytosolic $[Ca^{2+}]_i$

Q2 576 Repetitive increases of cytosolic $[Ca^{2+}]_i$, also referred to as
577 Ca^{2+} , oscillations represent a nearly universal signalling
578 mechanism in non-excitable cells by reducing the threshold
579 for the activation of calcium-dependent transcription factors
580 such as NFAT, NF- κ B or CREB [8] and by modulating protein
581 kinase activity [26, 34]. Ca^{2+} oscillations have been reported
582 in a great variety of non-excitable cells including pancreatic
583 β -cells [49], embryonic stem cells (ESCs) [47], chondroblasts
584 [11, 35], chondrocytes [40] and human MSCs [22, 24]. This is
585 the first study to report that human chondroprogenitor cells
586 derived from regions with minor lesions of osteoarthritic
587 articular cartilage (CPCs) are also characterised by a similarly
588 dynamic Ca^{2+} homeostasis. It is of note that these cells were
589 immortalised by viral transfection of hTERT and are
590 characterised by continuous proliferation under monolayer
591 culturing conditions applied in these experiments. Neverthe-
592 less, the chondrogenic potential of these cells has been dem-
593 onstrated [25]; and here, we present data that the mRNA
594 expression of various osteochondrogenic lineage markers
595 was detectable in CPCs. In contrast to embryonic chicken
596 limb bud-derived chondrogenic cells where high-frequency
597 (8×10^{-2} Hz) Ca^{2+} oscillations could be detected during fluo-
598 rescent single cell Ca^{2+} measurements [11, 53], CPCs exhib-
599 ited less frequent (1.3×10^{-3} Hz) periodic increases in $[Ca^{2+}]_i$,
600 similar to what has been described in MSCs [24, 50]. Like-
601 wise, Ca^{2+} oscillations in CPCs proved to be driven by inter-
602 nal Ca^{2+} stores as they could still be detected in Ca^{2+} -free
603 medium, with decreasing amplitudes. Noteworthy that rapid
604 Ca^{2+} oscillations in embryonic chicken limb bud-derived
605 chondroprogenitor cells were primarily mediated by extracel-
606 lular Ca^{2+} , probably due to their much smaller internal Ca^{2+}
607 stores [11, 53].

608 Functional characterisation of internal Ca^{2+} stores 609 and their role in generating Ca^{2+} oscillations

610 Next, we analysed the presence and function of ER-related
611 Ca^{2+} -signalling mechanisms. In terms of the two major Ca^{2+}
612 release channels of the ER, CPCs share homology with MSCs
613 wherein all IP₃R subtypes but no RyR isoforms are expressed
614 [24, 50], as opposed to chicken limb bud-derived
615 chondroprogenitor cells wherein only IP₃R1 could be detected
616 [33]. ESCs, on the other hand, are known to express all three
617 IP₃R subtypes [19], as well as RyRs [47]. The fact that CPCs
618 express all three IP₃R subtypes is not surprising as IP₃Rs are
619 known to be key components of Ca^{2+} oscillations and most
620 cells and tissues examined possess more than one subtype. In
621 fact, the properties of Ca^{2+} oscillation patterns depend on the
622 relative expression levels of IP₃R subtypes, probably because

of their specific response to endogenous modulators, such as
IP₃, Ca^{2+} and ATP. Pertaining to Ca^{2+} oscillations, IP₃R2 is
required for robust, long-lasting and regular Ca^{2+} oscillations;
IP₃R1 mediates less regular Ca^{2+} oscillations; and given that
IP₃R3 is the least sensitive to IP₃ as well as to Ca^{2+} , it
generates only monophasic Ca^{2+} transients [37, 54]. Contri-
bution from all IP₃R subtypes is likely necessary for the
characteristics (frequency, amplitude, amount of liberated
 Ca^{2+} , etc.) of Ca^{2+} oscillations in CPCs.

The indispensable role of IP₃R-mediated Ca^{2+} release from
internal Ca^{2+} stores in the generation of cytosolic Ca^{2+} oscil-
lations was further supported by the fact that application of the
aspecific IP₃R blocker 2-APB during single cell Ca^{2+} mea-
surements completely abolished spontaneous Ca^{2+} events.
These results are in perfect agreement with what has been
observed in MSCs [19, 23, 24] and also in ESCs [19], sug-
gesting that this might be a universal mechanism in the gen-
eration of Ca^{2+} oscillations in stem cells. Moreover, we pro-
vided evidence that SOCE was also essential for Ca^{2+} oscil-
lations in CPCs.

Our hypothesis that Ca^{2+} oscillations in CPCs were pre-
dominantly dependent on Ca^{2+} release through IP₃R followed
by store replenishment via SOCE was supported by key data
showing that the amount of Ca^{2+} liberated during spontaneous
 Ca^{2+} oscillations was almost identical to Ca^{2+} released during
CPA-induced store depletion. To our best knowledge, such an
intimate interrelation between Ca^{2+} oscillations and the Ca^{2+}
content of internal Ca^{2+} stores has not been documented in
stem cells.

The important role of SOCE in the Ca^{2+} homeostasis as
well as the presence of STIM1 and Orai1 in MSCs have been
documented [17, 24]; furthermore, the requirement of SOCE
to rapid Ca^{2+} oscillations along with STIM1, STIM2 and
Orai1 expressions have also been reported in chicken
chondroprogenitor cells [11]. The fact that CPCs express only
the STIM1 subtype may have important functional conse-
quences, for STIM2 is known to respond to smaller decreases
in the ER Ca^{2+} content (EC_{50} =406 mM vs. 210 mM for
STIM1), and therefore, it is the primary isoform that gets
activated at the initial steps of store depletion, while STIM1
only becomes active once the stores are almost fully emptied
[16]. Given that a considerable amount of Ca^{2+} is released
during each spontaneous transient from the internal stores, it is
primarily STIM1 that may play a determining role in trigger-
ing Orai isoforms [1].

As far as Orai isoforms are concerned, we confirmed that
CPCs express Orai1 proteins only. The fact that Orai1 and
Orai2 share many similarities may explain why CPCs are
devoid of that isoform [16]. Lack of Orai3, an essential
component of the store-independent, arachidonic acid-
regulated Ca^{2+} (ARC) channels, raises the possibility that
ARC channels are also absent from these cells [36]. The
distinct properties of Orai isoforms have recently been

reviewed by Hoth and Niemeyer [16]. However, a detailed characterisation of the precise role of STIM1 and Orai1 and their function in generating Ca^{2+} oscillations and their potential consequences of lineage-specific differentiation of CPCs require further analyses.

Purinergic signalling in CPCs and autocrine/paracrine regulation of Ca^{2+} oscillations

Ca^{2+} oscillations in human MSCs have been reported to be driven by an autocrine/paracrine purinergic loop, whereby ATP released through hemi-gap junctions triggered P2Y_1 metabotropic purinergic receptors and associated PLC- β and IP_3R signalling [22]. More recently, we have implicated a similar autoregulatory pathway in differentiating cells of chicken chondrogenic cell cultures, with P2X_4 ionotropic purinergic receptor being the most likely candidate [10, 11]. Given that CPCs were originally derived from OA-affected articular cartilage wherein extracellular nucleotides released along with inflammatory mediators may be considered as important ligands of purinergic receptors [41], we aimed to study whether CPCs were able to respond to nucleotide stimulation by P1 and/or P2 receptor activation.

First, we established the P1 purinergic receptor profile of CPCs, which correlated well with that of MSCs as they are reported to express A_1 [7], $\text{A}_{2\text{A}}$ [21] and $\text{A}_{2\text{B}}$ [46], but no A_3 receptors. In particular, A_1 and $\text{A}_{2\text{B}}$ receptor-mediated signalling is known to be required for osteogenic differentiation of MSCs [7, 48]. In a different study, Gharibi and colleagues demonstrated that the activation of $\text{A}_{2\text{B}}$ receptors was required for the osteogenic gene induction of MSCs, whereas adipogenic differentiation was accompanied by significant increases in A_1 and $\text{A}_{2\text{A}}$ receptor expression [12]. The same P1 receptor subtypes were found to be expressed in articular chondrocytes [45]. The ability of A_1 purinoreceptors to induce differentiation towards various lineages may reflect on specific intracellular downstream mechanism linked to distinct P1 receptor subtypes. For further details, the authors refer the reader to a recently published review article in this field [5].

Next, we analysed the P2 purinergic receptor expression in CPCs. Ca^{2+} transients elicited by extracellular ATP administration during fluorescent single cell Ca^{2+} measurements were significantly smaller in Ca^{2+} -free medium compared to normal Ca^{2+} -containing solution as shown in Table 2, suggesting the involvement of both P2X and P2Y receptor isotypes. By

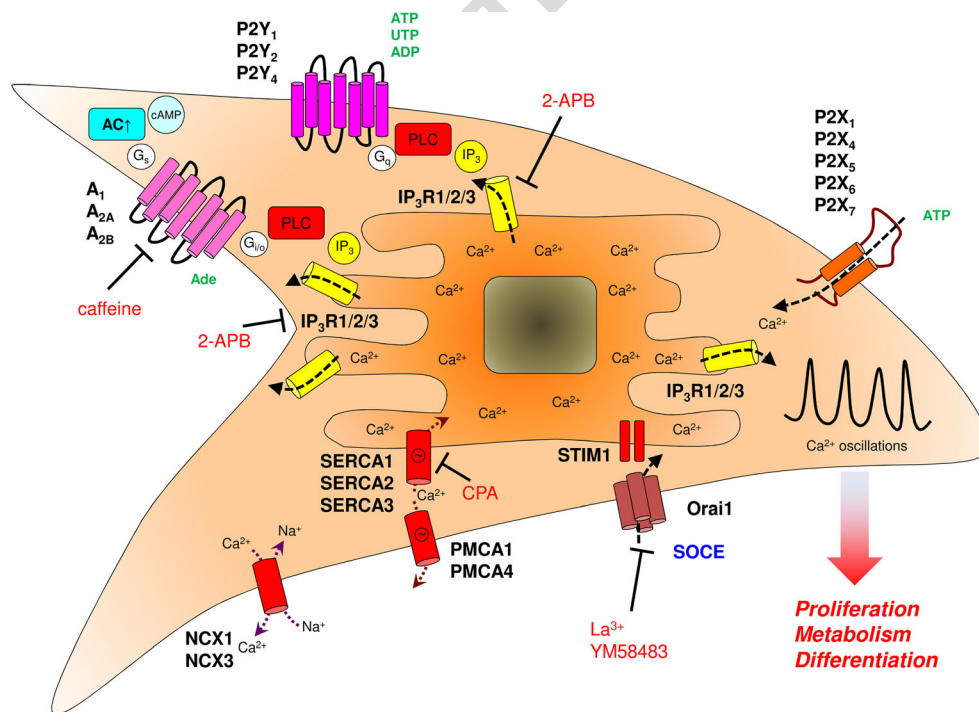


Fig. 5 Diagrammatical representation of molecular components of the Ca^{2+} toolkit verified in immortalised CPCs. Two main types of Ca^{2+} channels were identified; P2X ionotropic purinergic receptors and Orai1 CRAC channels. Of the two types of Ca^{2+} release channels, only $\text{IP}_3\text{R}1$, 2 and 3 were verified, but no RyR expression and function was detected. Metabotropic P1 and P2Y receptor subtypes coupled to Ca^{2+} release were also identified. All three major Ca^{2+} elimination pathways (SERCA, PMCA, NCX) were detected at least at the mRNA level. STIM1 ER Ca^{2+} sensor protein was verified, and the functionality of SOCE was also

recorded. Ca^{2+} oscillations are driven by external nucleotide (ATP) stimulation and maintained by Ca^{2+} release through IP_3R subtypes and subsequent Ca^{2+} influx (SOCE). Extracellular nucleotides may be released by CPCs in vitro and/or along with inflammatory mediators in osteoarthritic articular cartilage in vivo where other cell types can also be the source of their release (e.g. synovial cells; see [29]). Ca^{2+} oscillations may regulate proliferation, metabolic activity and differentiation of CPCs. Receptor agonists are shown in green, and antagonists are in red colour

contrast, when ATP was co-applied with the IP₃R inhibitor 2-APB, the majority of cells was unresponsive, implying that the primary mediators of extracellular nucleotides were metabotropic P2Y receptors. However, due to the apparent aspecificity of this inhibitor, the contribution of P2X receptors cannot be fully excluded [2]. By using various P2 receptor agonists (ATP, ADP, UTP and UDP; see Table 2 and [18]), as well as the non-specific receptor antagonist suramin, our results suggest the function of P2Y₁, P2Y₂, P2Y₄, P2X₄ and P2X₆ receptor subtypes in CPCs. These results are in a very good correlation with the findings of Zippel and colleagues who implicated the P2 receptor subtypes P2X₆, P2Y₄ and P2Y₁₄ to be key regulators in MSC commitment [55]; most of these receptors were active also in CPCs. Furthermore, these P2 receptor subtypes were found to be regulated during both adipogenic and osteogenic differentiation [55], implying a similar role of purinergic receptors in the differentiation of CPCs. The purinergic concept of MSC differentiation was further supported by the recently published results of Ciciarello and colleagues, who demonstrated that adipogenic differentiation of MSCs was mainly mediated by P2Y₁ and P2Y₄ receptors, while stimulation of the A_{2B} adenosine receptor subtype was primarily involved in osteogenic differentiation [6]. Given that CPCs can differentiate to osteogenic, adipogenic and chondrogenic lineages [25], their P1 and P2 receptor profile is in good correlation with the above data.

Purinergic receptors are known to mediate Ca²⁺ oscillations in various cell types [10, 13, 22, 28]. In this work, we propose that purinergic signalling may be the main drive Ca²⁺ of oscillations in CPCs as (1) breakdown of extracellular ATP and ADP by apyrase was able to completely abrogate Ca²⁺ oscillations and (2) the very same P2 purinergic receptors (i.e. P2X₄, P2Y₁) known to be key regulators of ATP-driven Ca²⁺ oscillations in MSCs and chondroprogenitor cells were functional also in these cells. Furthermore, the requirement of Ca²⁺ oscillations for the differentiation of CPCs is likely as the differentiation of MSCs has been reported to be directly influenced by both the application of P2 receptor agonists/antagonists and apyrase-induced nucleotide cleavage [55]. This, however, was beyond the scope of the current work and is yet to be determined.

Conclusions and perspectives

This is the first study to provide a functional characterisation of the Ca²⁺ toolkit in migratory chondroprogenitor cells derived from osteoarthritic cartilage (Fig. 5). It must be noted that the chondrogenic progenitor cell population (CPCs), which served as the cellular source of investigations described in this study, have been artificially immortalised by lentiviral introduction of the hTERT gene. Still, this cell population has been shown to undergo chondrogenic differentiation under appropriate culturing conditions [25]. In this paper, we provided evidence that CPCs are characterised by a dynamic Ca²⁺

homeostasis; we concluded that an extensive purinergic receptor array may drive Ca²⁺ oscillations that also intimately rely on Ca²⁺ release from internal Ca²⁺ stores through IP₃R subtypes and store refilling via SOCE. In many ways, the Ca²⁺ homeostasis of CPCs exhibit an intermediate stage between MSCs and chondroblasts/osteoblasts, which sets them apart from these cell populations. The P1 and P2 purinoreceptor profiling of CPCs revealed that they functionally express many receptor subtypes that are known to be involved in regulating Ca²⁺ oscillations and subsequent activation of transcription factors (e.g. NFAT, CREB), as well as commitment towards various lineages, metabolic activity and proliferation. Thus, the molecular components of the Ca²⁺ signalling toolkit identified in this work (Fig. 5) may provide CPCs with a framework that controls their commitment and subsequent differentiation. It is plausible to assume that through the activation of Ca²⁺ and other ion channels, Ca²⁺ signalling eventually converges on transcription factors such as Sox9 and/or Runx2, as well as proliferation. Such a connection has been verified during chondrogenesis [10, 11, 39, 51].

Given that OA is a currently incurable disease, any attempt to hinder or reverse disease progression and thus augment symptoms of millions of patients suffering from this condition are of utmost importance. To develop novel, targeted therapeutic approaches, a better understanding of the cellular background of the disease is inevitable. Notwithstanding their chondrogenic potential, CPCs fail to differentiate into chondroblasts in situ to initiate repair, probably owing to the non-permissive milieu of inflammatory cartilage. Having provided a detailed description on important aspects of Ca²⁺ signalling in CPCs, targeted alterations of their signal transduction pathways may enable us to exploit their chondrogenic differentiation potentials.

Acknowledgments We are grateful to Mrs. Krisztina Bíró and Mrs. Róza Óri for the excellent and skillful technical assistance. This work was supported by grants from the Hungarian Science Research Fund (OTKA CNK80709, OTKA NN-107765), from TÁMOP-4.2.2.A-11/1/KONV-2012-0036 and TÁMOP-4.2.2/B-10/1-2010-0024 projects, co-financed by the European Union and the European Social Fund. N.M. was supported by the German Research Foundation (Mi 573/10-1). C.M. was supported by a Mecenatura grant (DEOEC Mec-9/2011) from the Medical and Health Science Centre, University of Debrecen, Hungary; a Short-Term Fellowship from the Federation of European Biochemical Societies (FEBS); and also from the European Union through a Marie Curie Intra-European Fellowship for career development (project number: 625746; acronym: CHONDRION; FP7-PEOPLE-2013-IEF). This paper was supported by the János Bolyai Research Scholarship of the Hungarian Academy of Sciences. T.J. is supported by a Magyar Zoltán postdoctoral fellowship through the project entitled "National Excellence Program—Elaboration and implementation of a national student and researcher supporting system for the convergence region" (TÁMOP 4.2.4.A/2-11-1-2012-0001), co-financed by the Hungarian State, the European Union, and the European Social Fund.

Conflict of interest All authors disclose that there are neither any financial nor any personal relationships with other people or organisations

that could inappropriately influence (bias) their work. There are no conflicts of interests.

References

- Bird GS, Hwang SY, Smyth JT, Fukushima M, Boyles RR, Putney JW Jr (2009) STIM1 is a calcium sensor specialized for digital signaling. *Curr Biol* 19(20):1724–1729. doi:10.1016/j.cub.2009.08.022
- Bootman MD, Collins TJ, Mackenzie L, Roderick HL, Berridge MJ, Peppiatt CM (2002) 2-aminoethoxydiphenyl borate (2-APB) is a reliable blocker of store-operated Ca^{2+} entry but an inconsistent inhibitor of InsP_3 -induced Ca^{2+} release. *FASEB J* 16(10):1145–1150. doi:10.1096/fj.02-0037rev
- Burnstock G (2007) Purine and pyrimidine receptors. *Cell Mol Life Sci* 64(12):1471–1483. doi:10.1007/s00018-007-6497-0
- Bygrave FL, Benedetti A (1996) What is the concentration of calcium ions in the endoplasmic reticulum? *Cell Calcium* 19(6):547–551
- Carroll SH, Ravid K (2013) Differentiation of mesenchymal stem cells to osteoblasts and chondrocytes: a focus on adenosine receptors. *Expert Rev Mol Med* 15:e1. doi:10.1017/erm.2013.2
- Ciciarello M, Zini R, Rossi L, Salvestrini V, Ferrari D, Manfredini R, Lemoli RM (2013) Extracellular purines promote the differentiation of human bone marrow-derived mesenchymal stem cells to the osteogenic and adipogenic lineages. *Stem Cells Dev* 22(7):1097–1111. doi:10.1089/scd.2012.0432
- D'Alimonte I, Nargi E, Lannutti A, Marchisio M, Pierdomenico L, Costanzo G, Iorio PD, Ballerini P, Giuliani P, Caciagli F, Ciccarelli R (2013) Adenosine A1 receptor stimulation enhances osteogenic differentiation of human dental pulp-derived mesenchymal stem cells via WNT signaling. *Stem Cell Res* 11(1):611–624. doi:10.1016/j.scr.2013.04.002
- Dolmetsch RE, Lewis RS, Goodnow CC, Healy JL (1997) Differential activation of transcription factors induced by Ca^{2+} response amplitude and duration. *Nature* 386(6627):855–858. doi:10.1038/386855a0
- Ferrero ME (2009) A new approach to the inflammatory/autoimmune diseases. *Recent Pat Antiinfect Drug Discov* 4(2):108–113
- Fodor J, Matta C, Juhasz T, Olah T, Goncz M, Szigyarto Z, Gergely P, Csernoch L, Zakany R (2009) Ionotropic purinergic receptor P2X4 is involved in the regulation of chondrogenesis in chicken micromass cell cultures. *Cell Calcium* 45(5):421–430. doi:10.1016/j.ceca.2009.02.004
- Fodor J, Matta C, Olah T, Juhasz T, Takacs R, Toth A, Dienes B, Csernoch L, Zakany R (2013) Store-operated calcium entry and calcium influx via voltage-operated calcium channels regulate intracellular calcium oscillations in chondrogenic cells. *Cell Calcium* 54(1):1–16. doi:10.1016/j.ceca.2013.03.003
- Gharibi B, Abraham AA, Ham J, Evans BA (2011) Adenosine receptor subtype expression and activation influence the differentiation of mesenchymal stem cells to osteoblasts and adipocytes. *J Bone Miner Res* 26(9):2112–2124. doi:10.1002/jbmr.424
- Grierson JP, Meldolesi J (1995) Shear stress-induced $[\text{Ca}^{2+}]_i$ transients and oscillations in mouse fibroblasts are mediated by endogenously released ATP. *J Biol Chem* 270(9):4451–4456
- Gryniewicz G, Poenie M, Tsien RY (1985) A new generation of Ca^{2+} indicators with greatly improved fluorescence properties. *J Biol Chem* 260(6):3440–3450
- Harper MT, Poole AW (2011) Store-operated calcium entry and non-capacitative calcium entry have distinct roles in thrombin-induced calcium signalling in human platelets. *Cell Calcium* 50(4):351–358. doi:10.1016/j.ceca.2011.06.005
- Hoth M, Niemeyer BA (2013) The neglected CRAC proteins: Orai2, Orai3, and STIM2. *Curr Top Membr* 71:237–271. doi:10.1016/B978-0-12-407870-3.00010-X
- Hu J, Qin K, Zhang Y, Gong J, Li N, Lv D, Xiang R, Tan X (2011) Downregulation of transcription factor Oct4 induces an epithelial-to-mesenchymal transition via enhancement of Ca^{2+} influx in breast cancer cells. *Biochem Biophys Res Commun* 411(4):786–791. doi:10.1016/j.bbrc.2011.07.025
- Jacobson KA, Ivanov AA, de Castro S, Harden TK, Ko H (2009) Development of selective agonists and antagonists of P2Y receptors. *Purinergic Signal* 5(1):75–89. doi:10.1007/s11302-008-9106-2
- Kapur N, Mignery GA, Banach K (2007) Cell cycle-dependent calcium oscillations in mouse embryonic stem cells. *Am J Physiol Cell Physiol* 292(4):C1510–C1518. doi:10.1152/ajpcell.00181.2006
- Karlsson C, Dehne T, Lindahl A, Brittberg M, Pruss A, Sittinger M, Ringe J (2010) Genome-wide expression profiling reveals new candidate genes associated with osteoarthritis. *Osteoarthritis Cartilage* 18(4):581–592. doi:10.1016/j.joca.2009.12.002
- Katebi M, Soleimani M, Cronstein BN (2009) Adenosine A2A receptors play an active role in mouse bone marrow-derived mesenchymal stem cell development. *J Leukoc Biol* 85(3):438–444. doi:10.1189/jlb.0908520
- Kawano S, Otsu K, Kuruma A, Shoji S, Yanagida E, Muto Y, Yoshikawa F, Hirayama Y, Mikoshiba K, Furuichi T (2006) ATP autocrine/paracrine signaling induces calcium oscillations and NFAT activation in human mesenchymal stem cells. *Cell Calcium* 39(4):313–324. doi:10.1016/j.ceca.2005.11.008
- Kawano S, Otsu K, Shoji S, Yamagata K, Hiraoka M (2003) Ca^{2+} oscillations regulated by Na^{+} - Ca^{2+} exchanger and plasma membrane Ca^{2+} pump induce fluctuations of membrane currents and potentials in human mesenchymal stem cells. *Cell Calcium* 34(2):145–156
- Kawano S, Shoji S, Ichinose S, Yamagata K, Tagami M, Hiraoka M (2002) Characterization of Ca^{2+} signaling pathways in human mesenchymal stem cells. *Cell Calcium* 32(4):165–174
- Koelling S, Kruegel J, Imer M, Path JR, Sadowski B, Miro X, Miosge N (2009) Migratory chondrogenic progenitor cells from repair tissue during the later stages of human osteoarthritis. *Cell Stem Cell* 4(4):324–335. doi:10.1016/j.stem.2009.01.015
- Kupzig S, Walker SA, Cullen PJ (2005) The frequencies of calcium oscillations are optimized for efficient calcium-mediated activation of Ras and the ERK/MAPK cascade. *Proc Natl Acad Sci U S A* 102(21):7577–7582. doi:10.1073/pnas.0409611102
- Kurebayashi N, Ogawa Y (2001) Depletion of Ca^{2+} in the sarcoplasmic reticulum stimulates Ca^{2+} entry into mouse skeletal muscle fibres. *J Physiol* 533(1):185–199
- Kwon HJ (2012) Extracellular ATP signaling via P2X(4) receptor and cAMP/PKA signaling mediate ATP oscillations essential for prechondrogenic condensation. *J Endocrinol* 214(3):337–348. doi:10.1530/JOE-12-0131
- Loredo GA, Benton HP (1998) ATP and UTP activate calcium-mobilizing P2U-like receptors and act synergistically with interleukin-1 to stimulate prostaglandin E2 release from human rheumatoid synovial cells. *Arthritis Rheum* 41(2):246–255. doi:10.1002/1529-0131(199802)41:2<246::AID-ART8>3.0.CO;2-I
- Lorenzo P, Bayliss MT, Heinigard D (2004) Altered patterns and synthesis of extracellular matrix macromolecules in early osteoarthritis. *Matrix Biol* 23(6):381–391. doi:10.1016/j.matbio.2004.07.007
- Mankin HJ, Lippello L (1970) Biochemical and metabolic abnormalities in articular cartilage from osteoarthritic human hips. *J Bone Joint Surg Am* 52(3):424–434
- Martel-Pelletier J, Boileau C, Pelletier JP, Roughley PJ (2008) Cartilage in normal and osteoarthritis conditions. *Best Pract Res Clin Rheumatol* 22(2):351–384. doi:10.1016/j.berh.2008.02.001
- Matta C, Fodor J, Szigyarto Z, Juhasz T, Gergely P, Csernoch L, Zakany R (2008) Cytosolic free Ca^{2+} concentration exhibits a

- characteristic temporal pattern during in vitro cartilage differentiation: a possible regulatory role of calcineurin in Ca-signalling of chondrogenic cells. *Cell Calcium* 44(3):310–323. doi:10.1016/j.ceca.2007.12.010
34. Matta C, Mobasheri A (2014) Regulation of chondrogenesis by protein kinase C: emerging new roles in calcium signalling. *Cell Signal*. doi:10.1016/j.cellsig.2014.01.011
35. Matta C, Zakany R (2013) Calcium signalling in chondrogenesis: implications for cartilage repair. *Front Biosci* 5:305–324. Schol Ed
36. Mignen O, Thompson JL, Shuttleworth TJ (2009) The molecular architecture of the arachidonate-regulated Ca²⁺ -selective ARC channel is a pentameric assembly of Orai1 and Orai3 subunits. *J Physiol* 587(17):4181–4197. doi:10.1113/jphysiol.2009.174193
37. Miyakawa T, Maeda A, Yamazawa T, Hirose K, Kurosaki T, Iino M (1999) Encoding of Ca²⁺ signals by differential expression of IP₃ receptor subtypes. *EMBO J* 18(5):1303–1308. doi:10.1093/emboj/18.5.1303
38. Mobasheri A, Henrotin Y (2010) Identification, validation and qualification of biomarkers for osteoarthritis in humans and companion animals: mission for the next decade. *Vet J* 185(2):95–97. doi:10.1016/j.tvjl.2010.05.026
39. Muramatsu S, Wakabayashi M, Ohno T, Amano K, Ooishi R, Sugahara T, Shiojiri S, Tashiro K, Suzuki Y, Nishimura R, Kuhara S, Sugano S, Yoneda T, Matsuda A (2007) Functional gene screening system identified TRPV4 as a regulator of chondrogenic differentiation. *J Biol Chem* 282(44):32158–32167. doi:10.1074/jbc.M706158200
40. Nguyen C, Lieberherr M, Bordat C, Velard F, Come D, Liote F, Ea HK (2012) Intracellular calcium oscillations in articular chondrocytes induced by basic calcium phosphate crystals lead to cartilage degradation. *Osteoarthritis Cartilage* 20(11):1399–1408. doi:10.1016/j.joca.2012.07.017
41. Picher M, Graff RD, Lee GM (2003) Extracellular nucleotide metabolism and signaling in the pathophysiology of articular cartilage. *Arthritis Rheum* 48(10):2722–2736. doi:10.1002/art.11289
42. Piirainen H, Ashok Y, Nanekar RT, Jaakola VP (2011) Structural features of adenosine receptors: from crystal to function. *Biochim Biophys Acta* 1808(5):1233–1244. doi:10.1016/j.bbame.2010.05.021
43. Ralevic V, Burnstock G (1998) Receptors for purines and pyrimidines. *Pharmacol Rev* 50(3):413–492
44. Ramage L, Martel MA, Hardingham GE, Salter DM (2008) NMDA receptor expression and activity in osteoarthritic human articular chondrocytes. *Osteoarthritis Cartilage* 16(12):1576–1584. doi:10.1016/j.joca.2008.04.023
45. Rosenthal AK, Hempel D, Kurup IV, Masuda I, Ryan LM (2011) Purine receptors modulate chondrocyte extracellular inorganic pyrophosphate production. *Osteoarthritis Cartilage* 18(11):1496–1501. doi:10.1016/j.joca.2010.08.004
46. Ryzhov S, Goldstein AE, Novitskiy SV, Blackburn MR, Biaggioni I, Feoktistov I (2012) Role of A2B adenosine receptors in regulation of paracrine functions of stem cell antigen 1-positive cardiac stromal cells. *J Pharmacol Exp Ther* 341(3):764–774. doi:10.1124/jpet.111.190835
47. Sauer H, Hofmann C, Wartenberg M, Wobus AM, Hescheler J (1998) Spontaneous calcium oscillations in embryonic stem cell-derived primitive endodermal cells. *Exp Cell Res* 238(1):13–22. doi:10.1006/excr.1997.3809
48. Shih YR, Hwang Y, Phadke A, Kang H, Hwang NS, Caro EJ, Nguyen S, Siu M, Theodorakis EA, Gianneschi NC, Vecchio KS, Chien S, Lee OK, Varghese S (2014) Calcium phosphate-bearing matrices induce osteogenic differentiation of stem cells through adenosine signaling. *Proc Natl Acad Sci U S A* 111(3):990–995. doi:10.1073/pnas.1321717111
49. Stout CE, Costantin JL, Naus CC, Charles AC (2002) Inter-cellular calcium signaling in astrocytes via ATP release through connexin hemichannels. *J Biol Chem* 277(12):10482–10488. doi:10.1074/jbc.M109902200
50. Tao R, Sun HY, Lau CP, Tse HF, Lee HC, Li GR (2011) Cyclic ADP ribose is a novel regulator of intracellular Ca²⁺ oscillations in human bone marrow mesenchymal stem cells. *J Cell Mol Med* 15(12):2684–2696. doi:10.1111/j.1582-4934.2011.01263.x
51. Tian M, Duan Y, Duan X (2010) Chloride channels regulate chondrogenesis in chicken mandibular mesenchymal cells. *Arch Oral Biol* 55(12):938–945. doi:10.1016/j.archoralbio.2010.08.005
52. Varani K, De Mattei M, Vincenzi F, Tosi A, Targa M, Masieri FF, Pellati A, Massari L, Borea PA (2010) P2X(1) and P2X(3) purinergic receptors differentially modulate the inflammatory response in human osteoarthritic synovial fibroblasts. *Cell Physiol Biochem* 25(2–3):325–336. doi:10.1159/000276565
53. Varga Z, Juhasz T, Matta C, Fodor J, Katona E, Bartok A, Olah T, Sebe A, Csernoch L, Panyi G, Zakany R (2011) Switch of voltage-gated K⁺ channel expression in the plasma membrane of chondrogenic cells affects cytosolic Ca²⁺ -oscillations and cartilage formation. *PLoS One* 6(11):e27957. doi:10.1371/journal.pone.0027957
54. Zhang S, Fritz N, Ibarra C, Uhlen P (2011) Inositol 1,4,5-trisphosphate receptor subtype-specific regulation of calcium oscillations. *Neurochem Res* 36(7):1175–1185. doi:10.1007/s11064-011-0457-7
55. Zippel N, Limbach CA, Ratajski N, Urban C, Luparello C, Pansky A, Kassack MU, Tobiasch E (2012) Purinergic receptors influence the differentiation of human mesenchymal stem cells. *Stem Cells Dev* 21(6):884–900. doi:10.1089/scd.2010.0576

AUTHOR QUERIES

AUTHOR PLEASE ANSWER ALL QUERIES.

- Q1. Please provide significance for the items in *italic* (originally **bold**). Otherwise, please remove the emphasis.
- Q2. Please check if the edit to the sentence starting with "Repetitive increases of cytosolic $[Ca^{2+}]$, also referred to as Ca^{2+} , oscillations..." is correct or if the intended meaning of the text is retained.

UNCORRECTED PROOF